VOL. 11, NO. 6, MARCH 2016 ISSN 1819-6608
ARPN Journal of Engineering and Applied Sciences

www.arpnjournals.com

TRANSMISSION CHARACTERISTICS OF RING PERIODIC ARRAY FOR RADOME APPLICATIONS

S. Othman, N. K. A. Khalid and F. C. Seman
Wireless and Radio Science Centre, Faculty of Electrical and Electronic Engineering, Universiti Tun Hussein Onn Malaysia, Malaysia
E-Mail: fauziahs@uthm.edu.my

ABSTRACT

This paper investigates the transmission characteristics of ring loop FSS. Numerical study regarding the electrical characteristics using an equivalent circuit is developed. The FSS is optimized to operate between 8 to 12 GHz frequency range. The ring loop provides -10 dB bandwidth of 35 % (8-11.5 GHz). The simulated results are in good agreement with the measured results therefore validating the reliability of techniques using free space measurement. This provides additional guidelines for designing FSS with specified transmission characteristic for radome applications.

Keywords: ring patch, frequency selective surfaces, measurement technique.

INTRODUCTION

Frequency Selective Surfaces (FSSs) have been widely used in various applications such as dichroic reflector [Pasian *et al*., 2013], antenna radomes [Zhao and Xu, 2011], and electromagnetic filters [Sung *et al*., 2006]. There is large volume of published studies describing the function of the FSS as the bandpass [Kiani *et al*., 2011] or bandstop filters [Kiermeier and Biebl, 2007]. Filter characteristics of the FSS are mainly dependent on the surface's element pattern, conductivity of the element and properties of the substrate; therefore it is classified as a resonating element [Alkayyani and Qasem, 2013].

The ring loop element has great advantages due to its superior performance in terms of the stability under various angles of incidence, cross-polarization, bandwidth and level of band seperation [Unal *et al.*, 2006]. There are two common design approaches for designing a Frequency Selective Surfaces (FSS) which are numerical calculation based on commercially available software and equivalent circuit analysis [Ismail *et al.*, 2014]. Thus, in this study, a single ring loop FSS that exhibits excellent stability at normal and oblique incidence is proposed. The FSS is designed to attenuate signals operating at 10 GHz. Utilising commercial software is a preferable technique since it provides accurate simulated results however it consumes relatively more time to complete and involve licensing fee. Alternative option is utilizing equivalent circuit analysis, in which reflection and transmission characteristics are described by equivalent circuit model of lumped components resistor (R), Inductor (L) and Capacitor (C) based on the shape and size of physical structure of the FSS. It might be not as accurate as numerical simulation however it provides guidelines to the researchers the way especially dealing with a conventional type FSS elements. Somehow the results obtained from these two techniques can be linked together so any similarity/agreement could be observed.

RING PATCH FSS GEOMETRY AND DESIGN CONSIDERATION

FSS and equivalent circuit

The unit cell dimensions of ring loop FSS are shown in Figure-1. The ring loop is printed on dielectric substrate with the dielectric permittivity, ε_r=4.3 and thickness, t=1.6 mm. The effective dielectric permittivity is calculated as ε_{eff}=0.5(ε_r+1) [Munk, 2000]. The resonance frequency will decrease as the dielectric permittivity increases due to the loading effect of the dielectric [Kiermeier and Biebl, 2007]. Therefore, it is very crucial to take into account the dielectric properties of the substrate when designing the FSS.

Another important design parameters to consider is the dimensions of ring loop FSS. Generally, a ring loop FSS can be represented by a parallel equivalent circuit with a capacitive component in series with an inductive and a resistive[Sung *et al*., 2006] component as illustrated in Figure-1(c). The resonance frequency of the FSS is inversely proportional to $\sqrt{LC}$ in which contributed by the periodicity, length and width of the conductor loop.

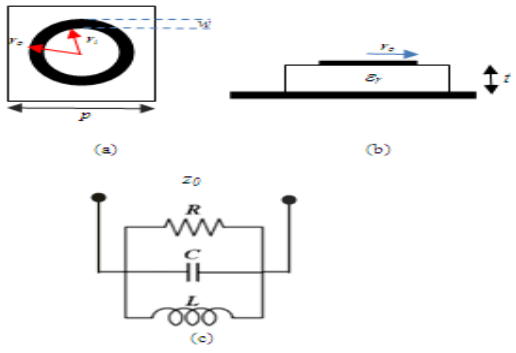

Figure-1. Unit cell of ring patch FSS (a) top view (b) side view (c) equivalent circuit.

Since the FSS is designed to reflect signals at 10 GHz, the values of capacitor (C), inductor (L) and resistor (R) can be obtained from equation (1), (2) and (3) as follows;

$$C = \frac{\pi}{z_o \omega_o} \quad (1)$$

$$L = \frac{\pi}{\omega_o^2 C} \quad (2)$$

$$R = \frac{z_o}{5.29 \times 10^{-3} \lambda_g} \quad (3)$$

Where z_o is the free space impedance, 377Ω and $\omega_o = 2\pi f_o$ and f_o is the operating frequency and $\lambda_g = 2\pi r_i$. At resonance frequency of the FSS, effective impedance of the FSS is perfectly matched to z_o therefore explaining the occurrence of RF signals attenuation.

Simulation Results

From equation (1) - (3) the electrical characteristics of the FSS equivalent circuit were determined based on the specified operating frequency. The proposed values of the equivalent circuit is mapped using Multisim software then the transmission characteristics of the FSS using equivalent circuit analysis can be observed. On the other hand, the commercially CST Microwave Studio is employed where the physical structures of w and r_i are changed accordingly. If both of the FSS resonant from Multim are matched to the one from CST, then the relationship on the R, C and L to w and r_i are performed. The resonant frequency (GHz) is found to be about the the same for both techniques however there will be slight different on the RF attenuation in dB at the centre FSS resonant.

In the first stage, the periodicity of the FSS elements, p is increased from 9 mm to 11 mm. The w and $r_i$is maintained to be 1 mm and 3.26 mm respectively. Figure-2 shows the relationship between the size of the periodicity, p with the values of capacitance and inductance. It can be seen that, both capacitance and inductance values decrease with the increase of p. The capacitance decreases by 0.018 pF as p increases from 9 mm to 11 mm. Similarly, the inductance reduces to 1.849 nH as the periodicity increases to 11 mm.

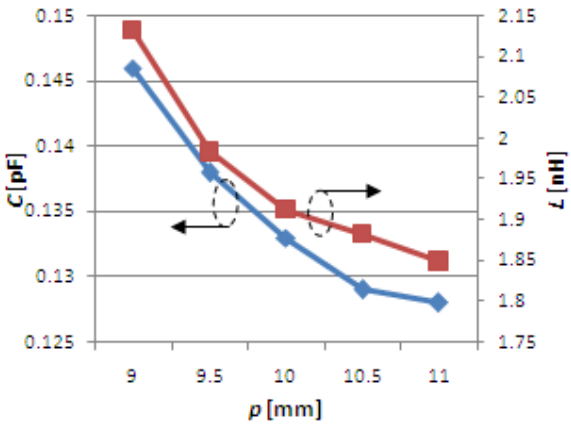

Figure-2. Capacitance and inductance versus periodicity.

In the second stage, the periodicity, p and r_o is fix at 10 mm and 4.26 mm respectively but the w is varied from 1.05 mm to 1.25 mm while r_i reduces from 3.21mm, 3.26mm, 3.11mm, 3.06mm dan 3.01mm. In order to investigate the relationship between the width of the element, $w$and r_i with the capacitance and inductance values, w is varied from 1.05 mm to 1.25 mm. Figure-3 (a) illustrates that both capacitance and inductance values decrease as w increases. When w equals 1.05 mm, capacitance and inductance are equal to 0.146 pF and 1.822 nH, respectively. However, as w increases up to 1.25 mm, capacitance decreases by 0.018 pF. Likewise, the inductance decreases to 1.722 nH when w equals 1.25 mm.

Equation 3 shows that the resistance is inversely proportional to the value of the internal radius, r_i of the ring loop FSS. In order to validate their relationship, as the internal radius, r_i reduces from 3.01 mm to 3.26 mm. As shown in Figure-3 (b), the resistance decreases linearly with the increases of internal radius. The resistance decreases from 3.77 KΩ to 3.48 KΩ as r_i increases up to 3.26 mm. Since f_o =10 GHz, the parameters of $C$and $L$are calculated as 0.133pF and 1.91 nH, respectively.

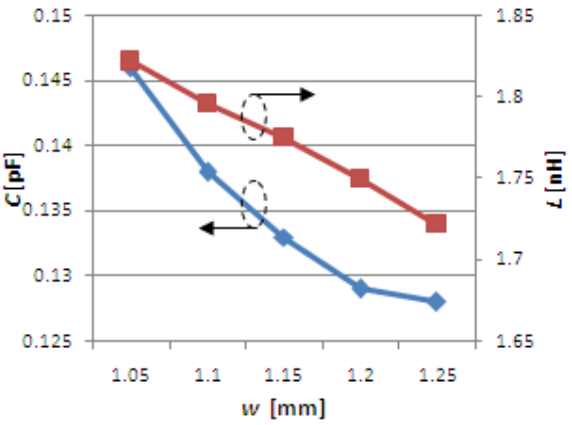

(a)

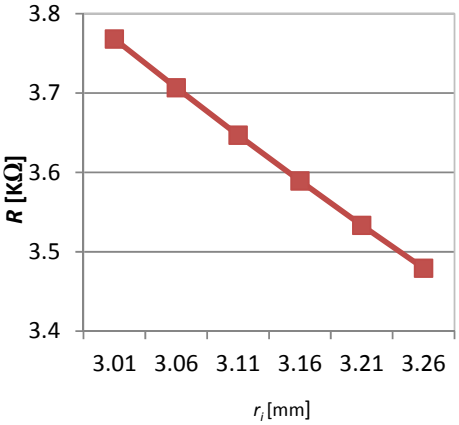

(b)

Figure-3. Capacitance and inductance versus (a) width (b) internal radius.

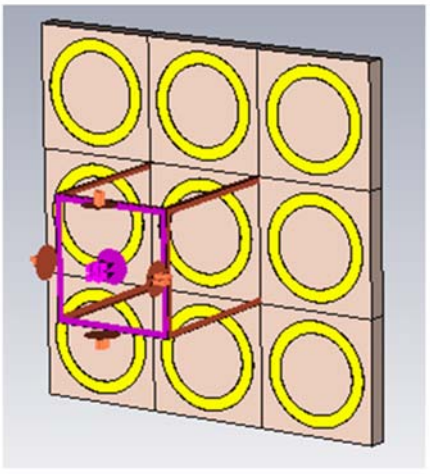

Figure-4. Periodic structure of the ring loop FSS.

CST RESULTS

CST provides better accuracy on the transmission plot results since they are offering full wave solver. Therefore the optimized dimension of the FSS operates at 10GHz was simulated by using the Computer Simulation Technology (CST) Microwave Studio software. The simulation is performed from 8-12 GHz by using the frequency domain solver. Unlike the time domain solver, the frequency domain solver is suitable for highly resonance structures and can be used to examine the angular stability of the designed FSS. The periodic boundary condition is chosen to represent an electrically large size of FSS radome working environment as shown in Figure-4. In order to tune the resonance frequency exactly at 10 GHz, the periodicity, p is optimized to 10 mm. Similarly, the external and internal radiuses of the FSS element are optimized to 4.26 mm and 3.26 mm, respectively.

The simulated transmission frequency response of ring loop FSS at normal incidence is illustrated in Figure-5. At the resonance frequency of 10 GHz, the proposed FSS provides a maximum attenuation of -35.12 dB. Besides, the designed FSS offers a great bandwidth performance of more than 35%.

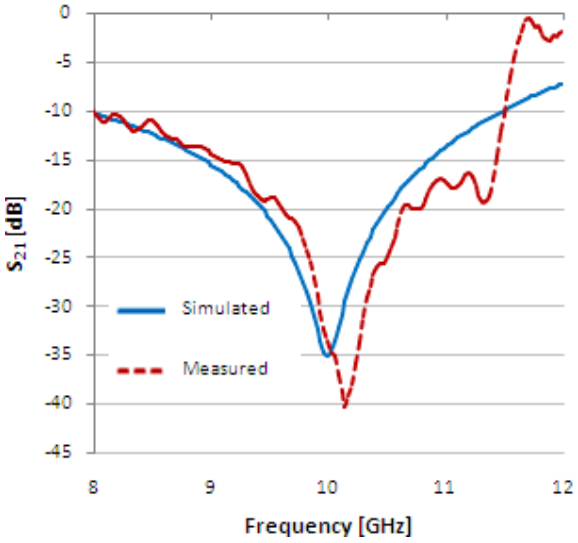

Figure-5. Simulated and measured transmission frequency response at normal incidence.

Fabrication and Measurement Technique

The proposed ring loop FSS was etched on FR-4 substrate with the thickness of 1.6 mm and loss tangent value of 0.025. A single-layer Printed Circuit Board (PCB) with one layer of copper foil was used since FSS does not require a ground plane. The fabricated prototype is shown in Figure 6 Due to the size limitation of the ultraviolet (UV) machine; the maximum possible size of the fabricated FSS is up to 30 cm x 30 cm. The dimension of the fabricated FSS was observed and the tolerance is found to be ±0.5 mm. Figure 6 shows the measurement setup that was carried out inside the anechoic chamber. The measurement setup consists of two horn antennas, fabricated FSS and network analyzer. The fabricated FSS was placed in the middle between the antennas that were

separated about 0.5 m away. The separation of the antennas must obey the far-field region Equation (4), where λ is the wavelength of the operating frequency and D is the horn antennas' maximum dimension [Raspopoulos and Stavrou, 2011].

$$d_{farfield} \geq \frac{2D^2}{\lambda} \quad (4)$$

The 15 dB transmitter and receiver horn antennas were connected to the network analyzer by using the coaxial cable. In order to measure the attenuation of the microwave signals that was contributed merely by the FSS, the loss due to the propagation path was taken out.

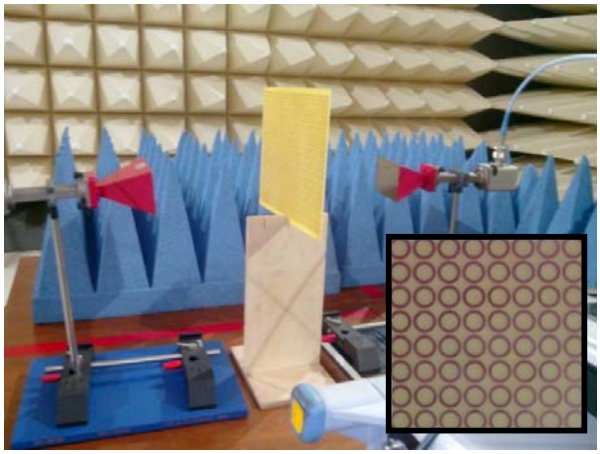

Figure-6. Free space measurement setup and fabricated ring loop FSS.

Figure-5 shows the measured transmission frequency response of the ring loop FSS. Generally, it can be seen that the simulated and measured transmission responses are in very good agreement with each other. The small deviation appears in the measured results is expected due to the scattering of the signals from the surroundings.

CONCLUSIONS

Analysis on equivalent circuit comprises of R, L and C with w, p and r_i is established. It is shown that R, L and $C$is inversely proportional to increment in size of physical structure of the FSS and this leads to reduction in the FSS resonant frequency. The performance of the ring loop FSS is demonstrated. The proposed FSS shows a superior performance in terms of the bandwidth with more that 35%. A minimumtransmision at 10 GHz with an attenuation of at least -35 dB is achieved. The measured result are shown to be in very good agreement with the simulated result.

REFERENCES

AlKayyani, H., and Qasem, N. 2013. Convoluted frequency selective surface wallpaper to block industrial, scientific, and medical radio bands inside buildings. American Academic and Scholarly Research Journal Special Issue. vol. 5, no. 3.

Ismail, M.Y., Inam, M., Misran, N. 2014. Characterization of resonant elements for passive and reconfigurable reflect array design. 2014 5th International Conference on Intelligent and Advanced Systems (ICIAS), pp. 1-5.

Munk, B. 2000. Frequency Selective Surfaces: Theory and Design. New York: Wiley.

Kiani, G., Olsson, L., Karlsson, A., Esselle, K. and Nilsson, M. 2011. Cross-dipole bandpass frequency selective surface for energy-saving glass used in buildings. IEEE Trans. Antennas and Propag. vol. 59, no. 2, pp. 520-525.

Kiermeier, K. and Biebl, E. 2007. New dual-band frequency selective surfaces for GSM frequency shielding. 37th Eur. Microwave Conference, pp. 222-225.

Pasian, M., Bozzi, M. and Perregrini, L. 2013. Accurate modeling of dichroic mirrors in beam-waveguide antennas. IEEE Trans. Antennas and Propag. vol. 61, no. 4, pp. 1931-1938.

Raspopoulos, M. and Stavrou, S. 2011. Frequency selective buildings through frequency selective surfaces. IEEE Trans. Antennas and Propag., vol. 59, no. 8, pp. 2998-3005.

Sung, G., Sowerby, K., Neve, M. and Williamson, A. 2006. A frequency-selective wall for interference reduction in wireless indoor environments. IEEE Antennas and Propag. Mag. vol. 48, no. 5, pp. 29-37.

Zhao, J. and Xu, X. 2011. Study of the effect of a finite FSS radome on a horn antenna. International Conference on Microwave Technology and Computational Electromagnetics (ICMTCE), pp. 74-76.